

UC Irvine

UC Irvine Previously Published Works

Title

Thermo-optical response of cartilage during feedback-controlled laser-assisted reshaping

Permalink

<https://escholarship.org/uc/item/2v98k45j>

Authors

Wong, Brian J
Milner, Thomas E
Anvari, Bahman
[et al.](#)

Publication Date

1997-05-22

DOI

10.1117/12.275069

Copyright Information

This work is made available under the terms of a Creative Commons Attribution License, available at <https://creativecommons.org/licenses/by/4.0/>

Peer reviewed

Thermo-Optical Response Of Cartilage During Feedback Controlled Laser-Assisted Reshaping

Brian J.F. Wong^{1,2}, Thomas E. Milner¹, Bahman Anvari^{1,3}, Alexander Sviridov⁴, Alexander Omel'chenko⁴, Victor Vagratashvili⁴, Emil Sobol⁴, and J. Stuart Nelson¹

¹Beckman Laser Institute and Medical Clinic, 1002 Health Sciences Road East, University of California Irvine, CA 92697

²Department of Otolaryngology- Head and Neck Surgery, 101 The City Drive Bld 25, Rt 81, University of California, Irvine, Orange, CA 92868

³Department of Engineering, Harvey Mudd College, Claremont, CA 91711

⁴Center for Technological Lasers, Russian Academy of Sciences, Troitsk, Moscow Region 142092, Russia

ABSTRACT

Cartilage undergoes characteristic deformation following laser irradiation below the ablation threshold. Measurements of surface temperature and integrated scattered light intensity were performed during laser irradiation. Porcine auricular cartilage (1-2 mm thickness) was irradiated with an Nd:YAG laser ($\lambda = 1.32 \mu\text{m}$) with varying dose (J/cm^2). Surface temperature was monitored using a single element HgCdTe infrared detector, responsive between 10-14 μm . A HeNe laser beam ($\lambda = 632.8 \text{ nm}$) was incident on the back surface of the cartilage specimen and fractional integrated back scattered light intensity was measured using an integrating sphere and a silicon photodiode. Laser irradiation (2W, $5.83\text{W}/\text{cm}^2$, 50 Hz PRR) was allowed to proceed until surface temperature reached 70°C . Cartilage deformation was observed in each instance. Integrated scattered light intensity reached a plateau before the peak temperature (70°) was reached. At increased laser power (10 W, $39.45 \text{ W}/\text{cm}^2$, 50 Hz PRR), a feedback controlled cryogen spray was used to maintain surface temperature below 50°C . A similar plateau response was also noted in integrated scattered light intensity. This signal may be used to optimize the process of stress relaxation in laser cartilage reshaping. Several clinical applications are discussed.

KEYWORDS

Cartilage, laser induced reshaping, Nd:YAG laser, plastic surgery, reconstructive surgery, stress relaxation

1.0 INTRODUCTION

1.1 Objectives

The plastic deformation of cartilage via laser-mediated stress-relaxation has been demonstrated ex-vivo with animal and human cartilage(1-9). Native cartilage can be reshaped into stable new geometries using laser irradiation without carbonization or ablation, and remain viable. In this study, laser assisted cartilage shaping was accomplished using a Nd:YAG laser while radiometric surface temperature [$S_C(t)$ ($^\circ\text{C}$)] and integrated scattered light intensity $I(t)$ were measured simultaneously. We attempted to determine whether $I(t)$ and $S_C(t)$ measurements could assist in optimizing laser cartilage reshaping. In addition, a feedback controlled cryogen spray cooling system was used to maintain surface

temperature below 50°C during prolonged laser irradiation and minimize thermal injury due to uncontrolled heating (10-12). Integrated scattered light intensity $I(t)$ was also measured and the fractional change $[\Delta I(t)/I_0]$ calculated.

1.2 Cartilage Molecular Structure

Cartilage is a complex macromolecular tissue composed of 80% water, 13% collagen (Type II), and 7% protein-polysaccharide (proteoglycans). The proteoglycans and collagen molecules are synthesized by the chondrocyte, the constitutive cell of cartilage tissue. Collagen Type II forms a rigid framework that encases large meshes of proteoglycan macromolecules (100 - 200 mD). Proteoglycans contain copious numbers of charged species (chiefly COO^- and SO_3^- moieties under physiologic pH) and in the collagen mesh are compressed approximately 20 times their native size in free solution. As a consequence, electrostatic repulsion exists between negatively charged ion species that is only partially balanced by free ions in solution (counter ions). This electrical imbalance results in an intrinsic tissue turgor termed the Donnan osmotic pressure(13-15). The extrinsic morphology of cartilage is determined by the interplay of these ionic forces, ion and fluid flow in the matrix, and the tensile properties of the collagen mesh(14, 15).

1.3 Importance of cartilage as an aesthetic and functional framework

Cartilage forms the framework for several key aesthetic and functional structures in the head, neck, and thorax. Cartilage grafts are routinely used in surgical reconstruction of auricular and nasal deformities, as well as tracheal and laryngeal defects. Surgery involving these structures is performed secondary to trauma, congenital malformation, or chronic illness. At present, autologous cartilage is harvested from the pinna of the ear, costal margin (rib) or nasal septum and used at heterotopic sites. In auricular, nasal, or tracheal reconstruction, the cartilage must be reshaped to conform to the anatomical defect. In practice, this is accomplished by carving or suturing the cartilage into complex shapes with steel or plastic stitches. These surgical attempts at cartilage reshaping necessitate the harvesting of excessive donor tissue and severely limit the extent of potential reconstructions. This is particularly true with laryngotracheal reconstruction in the neonate and pediatric populations where little cartilage is available for harvest.

1.4 Previous Work on Cartilage Reshaping

Surgical alteration of native cartilage shape has been attempted using a wide range of methods. In the 1960's, Fry introduced the concept of "interlocked stresses"(16, 17). When a flat sheet of cartilage was scored on one side and then allowed to soak briefly in solution, the tissue would curve with the concavity being on the side opposing the partial thickness incisions. Subsequent work by Fry demonstrated that this phenomenon was dependent on both the proteoglycans and collagen in the tissue. He looked at shape changes in cartilage in response to thermal denaturation. Laser induced cartilage reshaping was introduced by Sobol (1-3, 5-7) using radiation emitted at $\lambda = 10.6 \mu\text{m}$ (CO_2) and $\lambda = 2.12 \mu\text{m}$ (Holmium:YAG).

Sobol has suggested that the stress relaxation in cartilage induced by moderate heating is due to the redistribution of water and free ions within the complex cartilage matrix or change in proteoglycan structure. Cartilage undergoes a characteristic phase transformation at about 70° C (6). Laser irradiation can be used to heat cartilage in a precise manner that is primarily dependent on the wavelength, pulse duration, irradiance, and optical properties of the tissue (18). For thin cartilage sections, reshaping can be induced

using a CO₂ laser at an irradiance of 50-70 W/cm² with a total energy dose between 1200 - 1800 J/g(6). For thick specimens, the Holmium:YAG laser was found to produce a near uniform temperature distribution in a 1 mm thick specimen at a fluence of 1.9 J/cm². Wang et al performed in vivo studies on a crushed canine trachea using a pulsed Nd:YAG laser ($\lambda = 1.44 \mu\text{m}$)(8, 9). Crushed tracheal cartilage was reshaped using an endoscopic approach. Cartilage and its overlying mucosa were simultaneously irradiated at a power density of 7 W/cm². Irradiation was stopped after a variable time period (5-6 minutes) determined by the decrease in tensile strength perceived by the surgeon using a surgical elevator holding the warped cartilage in a desired position and shape.

1.5 Spatially Selective Cooling of Laser Irradiated Tissues

Dynamic epidermal cooling using a cryogen spray has been used to minimize thermal damage to the skin surface while maximizing the destruction of subsurface structures in the treatment of port-wine stains (11). A large (~30-40°C) and rapid (10-40 ms) surface temperature reduction is obtained in response to millisecond cryogen spray application due to the liquid-vapor phase transition (12). A variation of this approach has been used for spatially selective photocoagulation in tissue using an infrared radiometry feedback system (10). Cryogen application can result in preservation of superficial regions with coagulative necrosis to the underlying tissue. In this study, a similar feedback controlled cryogen spray system is used to monitor and maintain cartilage surface temperature at a pre-determined level.

2.0. MATERIALS AND METHODS

2.1. Cartilage Specimens

Fresh porcine auricular cartilage was obtained immediately following euthanasia from a local abattoir (Clougherty Packing Company, Vernon, CA). The pinna of the ear was removed with a scalpel and the soft tissue including the perichondrium (Figure 1) was dissected leaving only the cartilaginous framework (Figure 2). Cartilage was stored in physiological saline and used immediately.

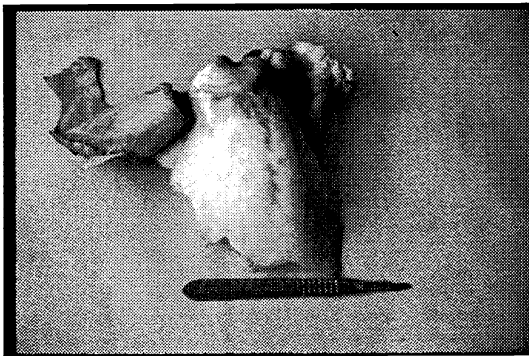


Figure 1: Porcine auricle with skin and periosteum still attached to cartilaginous framework at base. The scalpel blade is used as a size reference and measures six inches in length.

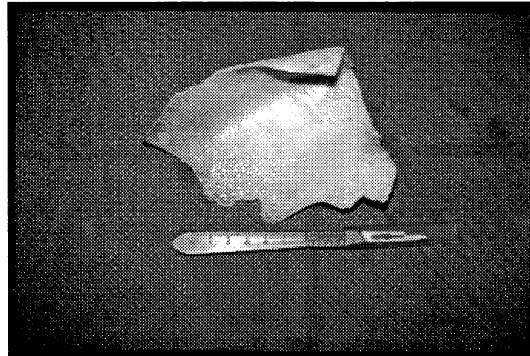


Figure 2: Porcine auricular cartilage completely stripped of soft tissue and perichondrium. The cartilage is thin and resilient.

Cartilage specimens were cut into rectangular shapes. Perichondrium was dissected free from the cartilage using a Freer elevator.

The thickness Δ_c of each specimen over the irradiated region was measured with a digital micrometer.

Cartilage specimens (flat in native state - Figure 3) were wrapped around a wooden dowel and secured in this position using steel pins (Figure 4). In contrast to

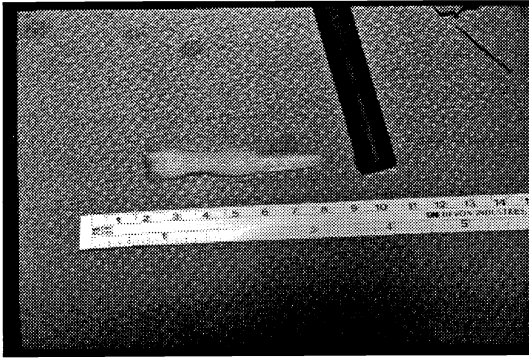


Figure 3: Native cartilage specimen before laser irradiation. The cartilage is flat and without curvature. The specimen is subsequently wrapped around a wooden dowel.

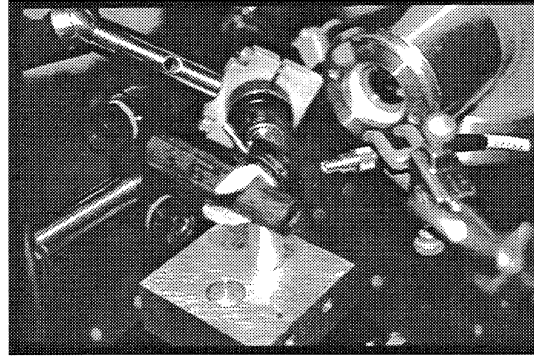


Figure 4: Cartilage specimen mounted on wooden dowel and secured in position with steel pins. Laser, cryogen cooling apparatus and IR detector are aimed toward the target site.

previous studies, laser irradiation was performed along the entire curved/stressed portion of the cartilage by rotating the specimen-dowel complex approximately

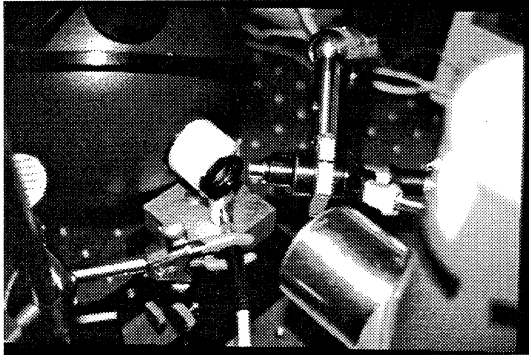


Figure 5 Cartilage specimen mounted on aperture. Laser, light scattering, and radiometric instrumentation surround the target site. A HeNe laser probe beam is directed onto the back surface of the cartilage specimen.

30° after each laser treatment. Radiometric surface temperature measurements were used to determine the duration of laser irradiation. For light scattering studies, specimens were suspended across the aperture bracket of the IR radiometry apparatus in a native configuration (flat) (see Figure 5).

2.2 Laser Parameters

Cartilage specimens were irradiated with a Nd:YAG laser ($\lambda = 1.32 \mu\text{m}$, 50 Hz PRR NewStar Lasers, Auburn, CA) with variable exposure time. Light was delivered by a 600 μm core-diameter silica multimode optical fiber. Laser power was determined using a pyroelectric meter (Model 10A-P, Ophir, Jerusalem, Israel). Laser spot size was estimated using thermal paper. Laser powers of 2 and 20 W were used for all Nd:YAG laser studies corresponding to power densities of 5.83 and 39.45 W/cm^2 respectively. Specimens were irradiated in the absence and presence of feedback controlled cryogen spray cooling. Light scattering and infrared radiometry measurements were simultaneously performed.

2.3 Temperature Measurement and Cooling Apparatus

Radiometric surface temperature [$S_c(t)$ ($^{\circ}\text{C}$)] was monitored using a 1 mm² liquid N₂ cooled HgCdTe detector (MDD-10E0-S1, Cincinnati Electronics, Mason, OH) as previously described(12)(Figure 6). The detector element was at the focal plane of a 25 mm diameter f/1 Ge lens, and was optically filtered by a 10-14 μm bandpass filter (RL-7500-F, Corion). The collection optics were configured for unit magnification with a 5 mm diameter exit pupil positioned 50 mm from the detector resulting in a f/10 system. The temperature of the detection system was calibrated with an aluminum block coated with highly emissive ($\epsilon=0.97$) black paint (TC-303 black, GIE Corp, Provo, Utah) heated from 23 to 100^o C by a resistive element. The surface temperature of the aluminum block was measured with a precision thermistor (8681, Keithley Instruments, Cleveland, OH) attached to the block. The radiometric signal at the center of the laser target site was used to trigger the delivery of cryogen spurts when the radiometric surface temperature reached a pre-specified value (50^o C). For cooling studies, a 40 ms cryogen spurt was delivered and repeated as necessary using the feedback controlled system.

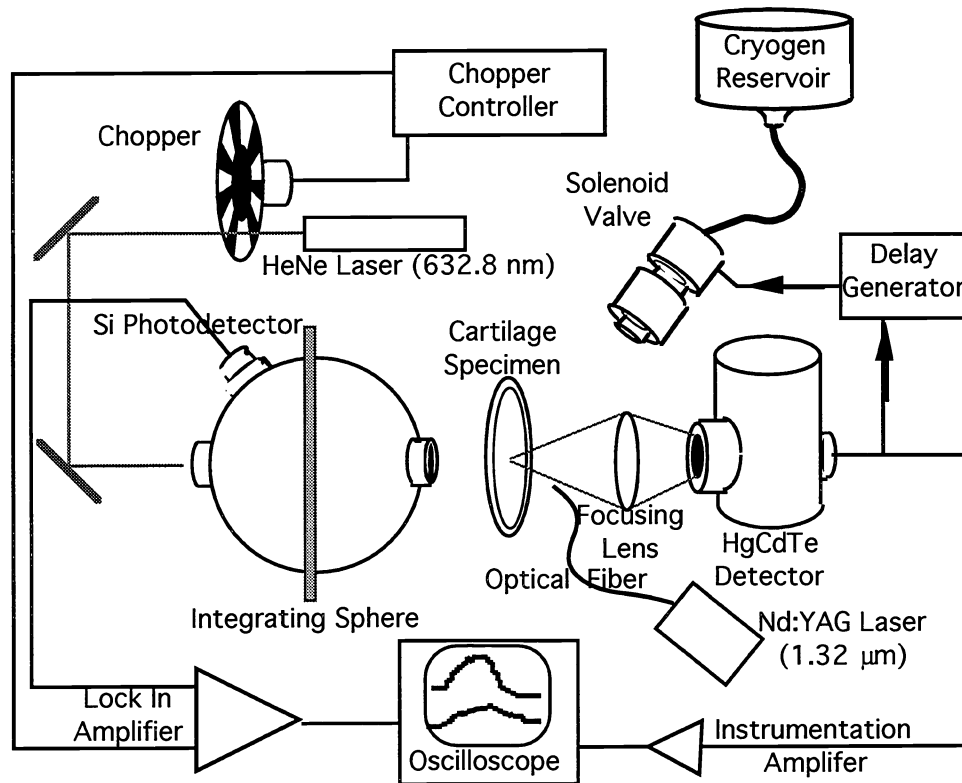


Figure 6: Schematic for light scattering, radiometric surface temperature measurements, and feedback controlled cryogen spray cooling . The cartilage specimen is secured on an mounting aperture at the focal point of the IR optical system. The HgCdTe IR detector, Nd:YAG laser, and cryogen cooling apparatus are directed toward the target site. The HgCdTe detector output is used as a feedback signal to control the cryogen cooling. A chopped HeNe laser beam is directed on the back surface of the cartilage specimen through an integrating sphere. A silicon photodiode measures the back-scattered light signal $I(t)$.

The test cryogen (Chlorodifluoromethane, boiling point $\sim 40^\circ\text{C}$, Aldrich Chemical Company, Milwaukee, Wisconsin) was stored in a pressurized ($\sim 5\text{ atm}$) steel canister. The cryogen was delivered by an electronically controlled standard automobile fuel injection valve (aperture diameter 1mm) creating a cooled region on the surface of the cartilage with a 7 mm diameter. The cryogen spurt duration (40 ms) was controlled by a programmable digital delay generator (DG 535, Stanford Research Systems, Sunnyvale, CA). Distance between the solenoid valve orifice and the cartilage surface was maintained at 20 mm.

2.4 Light Scattering Measurements

Back-scattered light from a HeNe laser ($\lambda_0 = 632.8\text{ nm}$, 15 mW, Melles Griot) incident on the non-irradiated surface of the cartilage specimen was collected in an integrating sphere (6", Labsphere, North Sutton, NH) and measured using a silicon photoreceiver (Model 2001, New Focus, Mountain View, CA) to yield integrated scattered light intensity $I(t)$ (Figure 5). In order to improve the signal to noise ratio, the HeNe laser intensity was amplitude modulated (1000 Hz) with a mechanical chopper (Model SR540, Stanford Research Systems) and synchronously detected by a lock-in amplifier (Model SR 850, Stanford Research Systems). The fractional change in integrated scattered light intensity $[\Delta I(t)/I_0]$ was calculated by measuring the change in $I(t)$ relative to the baseline signal I_0 prior to irradiation with the Nd:YAG laser. Both the scattered light signal and radiometric signals were displayed on a digital storage oscilloscope (Textronix DSA 601, Beaverton, OR).

3.0. RESULTS

The flat cartilage in Figure 3 was irradiated with the Nd:YAG laser which produced a marked curvature in the specimen (Figure 7) demonstrating the possibility of creating curved tracheal segments from a flat piece of cartilage.

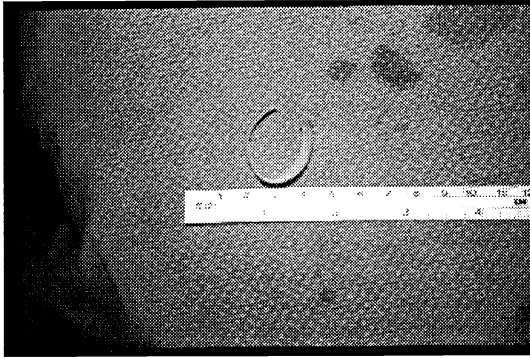
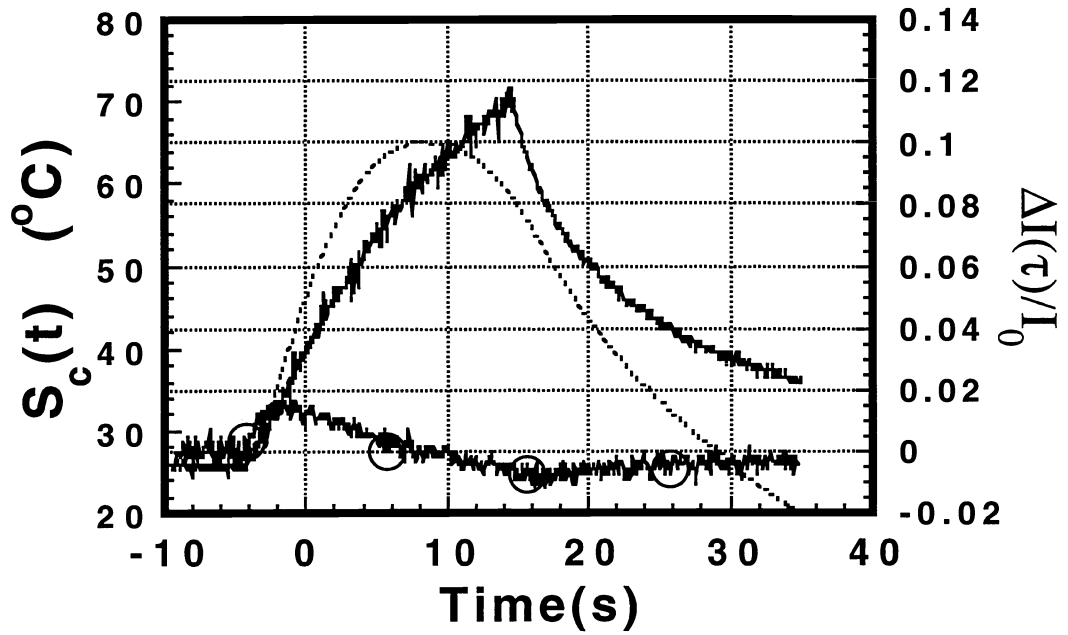


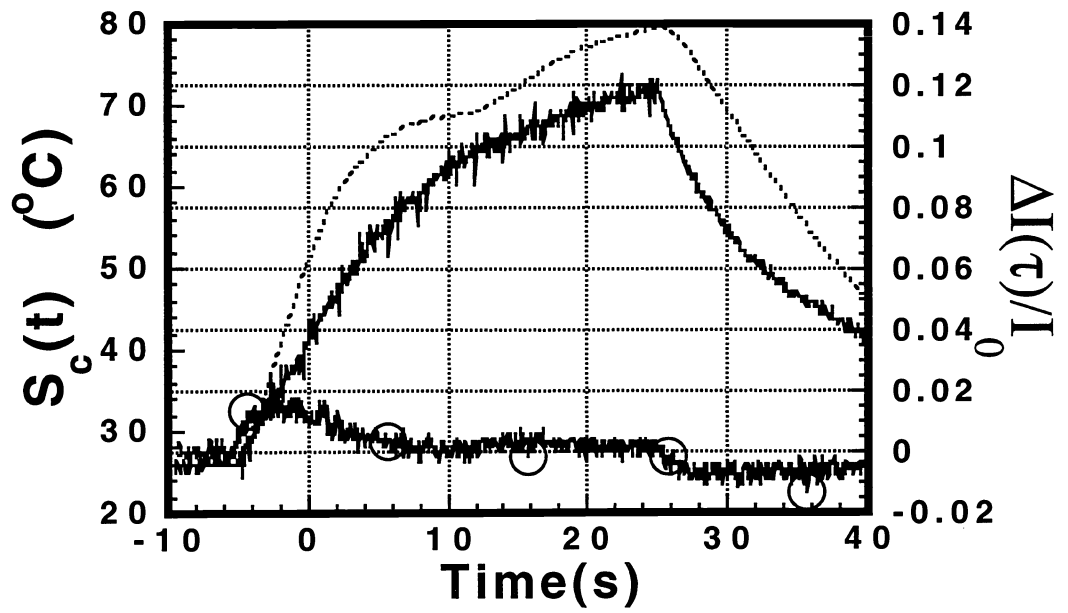
Figure 7: Laser shaped cartilage specimen following Nd:YAG laser irradiation. This is the same specimen as illustrated in Figure 3. Cryogen cooling was not used.

Figure 8 a-d depicts a series of plots corresponding to experiments where laser irradiance was moderate (slow temperature rise) (2W, 50 Hz PRR). Each figure represents a different cartilage specimen with thickness Δ_C varying between 1-2 mm. Laser spot size was 0.36 cm^2 corresponding to a power density of 5.83 W/cm^2 . Feedback controlled cooling was not employed and laser radiation was terminated when $S_C(t)$ reached approximately 70°C . The precise shape of $\Delta I(t)/I_0$ during heating appeared to be highly sensitive to cartilage position and varied between specimens. However the plateau region in the fractional change in intensity $[\Delta I(t)/I_0]$ occurred during the same

temperature interval ($65\text{-}70^\circ\text{C}$) for all specimens.

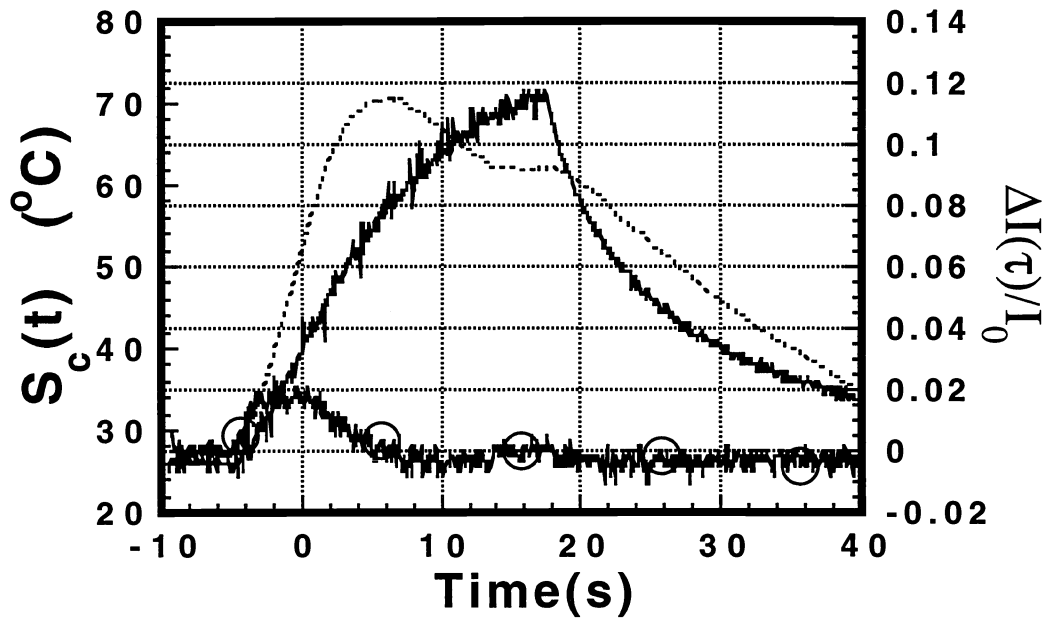


8 a

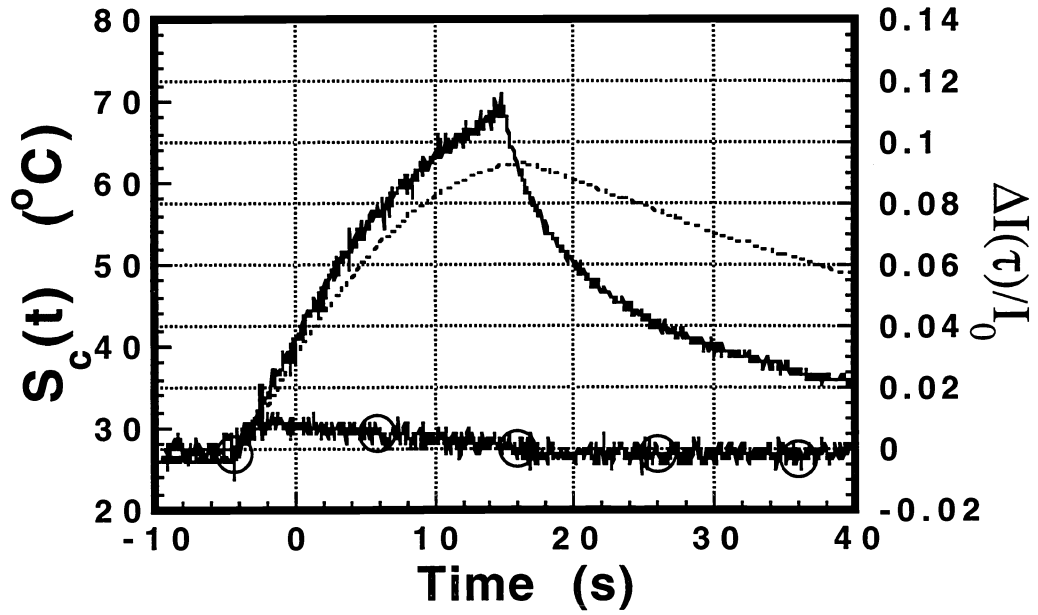


8 b

(legend on proceeding pages)



8 c



8 d

(legend on preceding pages)

Figure 8 a- d (on preceding pages) : Simultaneous measurements of radiometric surface temperature $S_c(t)$, fractional change in integrated scattered light intensity $\Delta I(t)/I_0$, and rate of change $(d(\Delta I(t)/I_0)/dt)$. The shape of $\Delta I(t)/I_0$ is highly variable and sensitive to specimen thickness and geometry, however the stationary region where $d(\Delta I(t)/I_0)/dt = 0$ remains constant. Zero slope for $\Delta I(t)/I_0$ consistently occurs during the temperature transition from 65-70°C. (a) the peak for $\Delta I(t)/I_0$ occurs prior to the 70°C threshold for tissue denaturation. (b) $\Delta I(t)/I_0$ assumes a biphasic shape yet retains the inflection change in the temperature interval between 65-70°C. (c) a biphasic shape for $I(t)/I_0$ is noted, though the peak occurs prior to the surface temperature reaching 70°C. (d) Temperature did not exceed 70°C in this specimen and the peak in $\Delta I(t)/I_0$ occurs after the temperature peak (at about 67°C). Laser radiation was stopped before $S_c(t)$ reached 70°C. (— $S_c(t)$, -.- $\Delta I(t)/I_0$, —○— $d(\Delta I(t)/I_0)/dt$).

In Figure 9, a specimen of fresh porcine auricular cartilage was irradiated for 4 seconds with the Nd:YAG laser operating at 10 W and 50 Hz. Laser spot size was 0.26 cm² corresponding to a power density of 39.45 W/cm². Application of three cryogen spray cooling spurts were required to maintain surface temperature below 50°C. Radiometric surface temperature [$S_c(t)$], the fractional change in integrated scattered light intensity [$\Delta I(t)/I_0$] and the time rate of change of $\Delta I(t)/I_0$ [$d(\Delta I(t)/I_0)/dt$] are depicted in the diagram. Note that $\Delta I(t)/I_0$ reaches a plateau at the same time laser irradiation terminates (as evidenced by the monotonic decline in $S_c(t)$).

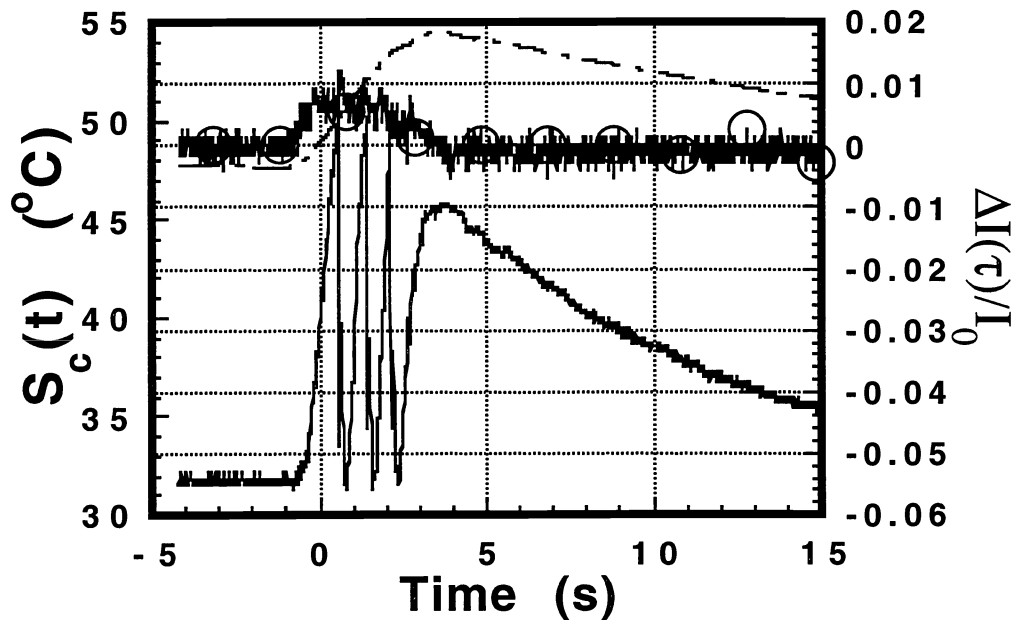


Figure 9: Feedback controlled laser assisted cartilage reshaping with cryogen spray cooling. Three cryogen spurts are initiated when radiometric surface temperature exceeds 50°C. The duration of the cryogen spurts was 40 ms. The scattered light signal peaks during the cessation of laser irradiation (— $S_c(t)$, -.- $\Delta I(t)/I_0$, —○— $d(\Delta I(t)/I_0)/dt$).

4.0 DISCUSSION

Laser assisted reshaping of native cartilage may provide a more effective means for morphologic and structural reconstruction than conventional surgical techniques. Several key elements of the technique require investigation before clinical application is considered. The first and foremost concern is cartilage viability. To date no "dose response" curves for cartilage viability following laser irradiation (below the ablation threshold) in healthy cartilage exist. Although limited histologic studies have been completed(9), the question is under investigation in our laboratory. Second, optimal laser parameters to mediate stress relaxation in cartilage are unknown. Undoubtedly, moderate heating (i.e., non-ablative energy densities) in combination with a feedback control system are necessary to minimize non-specific thermal injury.

Our preliminary measurements indicate that marked surface temperature elevations occur rapidly even with moderate power densities (Figure 8 a-d). The calculation of thermal injury is dependent on the spatial and temporal distribution of temperature as well as the light distribution in the tissue (19). As an estimate for tissue devitalization, we used a surface temperature threshold of 70° C (temperature at which irreversible protein denaturation occurs). With cryogen cooling, surface temperature may be maintained below an arbitrary temperature threshold. In Figure 9, $\Delta I(t)/I_0$ reaches a peak with the cessation of laser irradiation when surface temperature is kept below 50° C. We speculate that with prolonged irradiation (>30 s) and cryogen cooling, $\Delta I(t)/I_0$ would plateau and then decrease despite continued laser irradiation. We plan to perform this study while simultaneously measuring intrinsic stress in the cartilage specimen.

When feedback controlled cryogen spray cooling is employed, the surface temperature of the cartilage specimen can be maintained below a specified level. When the cryogen (boiling point ~ -40° C) contacts the target site, heat is liberated from the cartilage to the cryogen down a steep thermal gradient. The cryogen evaporates and the target site is rapidly cooled(12). As illustrated in Figure 9, three cryogen spurts were used to maintain the surface temperature below 50 °C during continuous pulsed Nd:YAG laser irradiation. While power densities used in this study did not create tissue coagulation or ablation, it is probable that subsurface temperature may exceed 70 °C in the presence of sustained moderate laser irradiation. Anvari et al. demonstrated that sub-surface temperature distribution in response to Nd:YAG laser irradiation with cryogen cooling may exceed 100°C in a coagulation model of tissue injury despite relatively low radiometric surface temperature measurements (10). In cryogen cooled cartilage reshaping, radiometric surface temperature measurements may be inadequate alone to predict tissue injury (sub-surface temperatures may exceed 100° C), and therefore $I(t)$ may be a more useful means to determine the critical point at which tissue undergoes the shape-phase transformation. For this reason, cooling was initiated at 50° C rather than 70° C to minimize this potential side effect of prolonged irradiation.

The fractional change in scattered light intensity $\Delta I(t)/I_0$ represents an estimate of the change in target site optical properties during laser irradiation and is dependent on both the light distribution of the HeNe probe beam (deeply penetrating in opaque tissues) and the Nd:YAG laser causing the temperature change. With moderate heating (and no cooling) $I(t)$ reaches a plateau when $S_C(t)$ is between 65-75° C as seen in Figure 8. Sobol et al(6) also observed this plateau effect in $I(t)$ (6). Although additional experiments are necessary to interpret the molecular basis of the light scattering results, the stationary region where

$d(\Delta I(t)/I_0)/dt = 0$ may correspond to the bound-to-free water phase transition hypothesized by Sobel(4). The phase transition begins by formation of local regions or "islands" of anomalous refractive index created when water bound to large proteoglycan molecules is liberated. In the theory of laser induced phase transitions (4), the "islands" are viewed as nucleation sites for a new phase. As the bound-to-free water phase transition nears completion, regions of anomalous refractive index become larger and eventually coalesce into a homogenous phase. The resultant change in slope needs to be identified during sustained laser irradiation with cryogen cooling and such studies are presently underway in our laboratories.

5.0 CONCLUSIONS

In summary, results of these studies demonstrate that the process of laser induced stress-relaxation in cartilage is accompanied, and may be monitored by observing changes in the fractional change of integrated scattered light intensity $\Delta I(t)/I_0$. Cryogen cooling may be a useful technique to allow rapid delivery of laser energy while simultaneously minimizing potential non-specific thermal injury. Radiometric surface temperature $S_c(t)$ may be less sensitive to the stress relaxation process in cartilage reshaping, but its measurement and control is necessary to minimize the side-effects of uncontrolled heating. Inasmuch as stress-relaxation is always accompanied by these changes, design of a feedback control system appears feasible. Nevertheless, since the correlation between observed changes and optimal laser irradiation parameters is not known, further laboratory experiments are needed to provide more information on the mechanism of laser-assisted cartilage reshaping.

The medical impact of this work would be most dramatic in airway and nasal reconstruction surgery. This work also has the potential for wide use in arthroplasty and in several orthopedic surgical procedures, particularly for changes due to trauma or rheumatologic disease.

6.0 ACKNOWLEDGMENTS

This work was supported by the Biomedical Research Technology Program, Institute of Arthritis and Musculoskeletal and Skin Diseases at the NIH, Whitaker Foundation, Dermatology Foundation, National Science Foundation, and the Research Fund of the American Otological Society.

7.0 REFERENCES

1. Helidonis E, Sobol E, Kavvalos G, et al. Laser Shaping of Composite Cartilage Grafts. American Journal of Otolaryngology 1993;14:410-412.
2. Helidonis A, Sobol E, Velegrakis G, Bizakis J. Shaping of Nasal Septal Cartilage with the Carbon Dioxide Laser- a Preliminary Report of an Experimental Study. Lasers in Medical Science 1994;9:51-54.
3. Sobol E, Bagratashvili V, Omel'chenko A, et al. Laser Shaping of Cartilage. Proceedings SPIE 1994;2128:43-49.
4. Sobol E. Phase transformations and ablation in laser-treated solids. New York: John Wiley, 1995

5. Sobol E, Bagratashvili V, Sviridov A, et al. Cartilage Reshaping with Holmium Laser. *Proceedings SPIE* 1996;2623:556-559.
6. Sobol E, Bagratashvili V, Sviridov A, et al. Phenomenon of Cartilage Shaping using Moderate Heating and its Application in Otorhinolaryngology. *Proceedings SPIE* 1996;2623:560-564.
7. Sobol E, Sviridov A, Bagratashvili V, et al. Stress Relaxation and Cartilage Shaping under Laser Radiation. *Proceedings SPIE* 1996;2681:358-363.
8. Wang Z, Pankratov MM, Perrault DF, Shapshay SM. Laser-Assisted Cartilage Reshaping: In vitro and in Vivo Animal Studies. *Proceedings SPIE* 1995;2395:296-302.
9. Wang Z, Pankratov MM, Perrault DF, Shapshay SM. Endoscopic Laser-Assisted Reshaping of Collapsed Tracheal Cartilage: A Laboratory study. *Annals of Otolaryngology, Rhinology, and Laryngology* 1996;105:176-181.
10. Anvari B, Tanenbaum BS, Milner TE, et al. Spatially selective photocoagulation of biological tissues: feasibility study utilizing cryogen spray cooling. *Applied Optics* 1996;35:3314-3320.
11. Nelson JS, Milner TE, Anvari B, et al. Dynamic Epidermal Cooling During Pulsed Laser Treatment of Port-Wine Stain. *Archives of Dermatology* 1995;131:695-700.
12. Anvari B, Milner TE, Tanenbaum BS, Kimel S, Svaasand LO, Nelson JS. Selective cooling of biological tissues: application for thermally mediated therapeutic procedures. *Physics in Medicine and Biology* 1995;40:241-252.
13. Donnan FG. The Theory of Membrane Equilibria. *Chemical Reviews* 1924;1:73-90.
14. Lai W, Hou J, Mow V. A triphasic theory for the swelling of hydrated charged soft biological tissues. In: Mow V, Ratcliffe A, Woo S-Y, ed. *Biomechanics of diarthroidal joints*. New York: Springer-Verlag, 1990: 283-312. vol 1,2).
15. Lai W, Hou J, Mow V. A Triphasic Theory for the Swelling and Deformation Behaviors of Articular Cartilage. *Journal of Biomechanical Engineering* 1991;113:245-258.
16. Fry H. Interlocked stresses in human nasal septal cartilage. *British Journal of Plastic Surgery* 1966;19:276-278.
17. Fry H. Cartilage and cartilage grafts: the basic properties of the tissue and the components responsible for them. *Plastic and Reconstructive Surgery* 1967;40:426-439.
18. Jacques SL. Role of tissue optics and pulse duration on tissue effects during high-power laser irradiation. *Applied Optics* 1993;32(13):2447-2454.
19. Pearce J, Thomsen S. Rate Process Analysis of Thermal Damage. In: Welch A, van Gemert M, ed. *Optical-Thermal Response of Laser-Irradiated Tissue*. New York: Plenum, 1995: 561-606.